INCREASED RBCC EJECTOR PERFORMANCE THROUGH AREA CONSTRICTION

Jason Etele*, Jean P. Sislian**
UTIAS

4925 Dufferin St., Toronto, ON, M3H 5T6, Canada
*jason@caius.utias.utoronto.ca, **sislian@caius.utias.utoronto.ca

Abstract

The present paper details the results of a study of several Rocket Based Combined Cycle engine ejector flow field configurations. Steady state solutions of the axisymmetric Favre averaged Navier-Stokes equations closed by the Wilcox kω turbulence model (including the Wilcox dilatational dissipation correction) are obtained using WARP, a finite difference flow solver using a Yee-Roe flux limiting scheme.

For a constant area ejector in which both the air and rocket exhaust mass flows are equal, compression ratios as high as 2.5 can be obtained using the combination of an annular and central rocket located along the outer wall and axisymmetric axis respectively (where the rocket exhaust mass flow is biased towards the annular stream by a ratio of 3:1). It is shown that this compression ratio can be increased 23% through a 25% constriction in the exit area over the entire length of the ejector. Further, the use of a conical/cylindrical configuration can increase the compression ratio by an additional 5%-7% over a purely conical configuration. This allows an overall increase of approximately 30% when compared to a constant area ejector under the same operating conditions.

1 Introduction

The importance of the space launch market to the global economy is manifest by the fact that in 2002 the satellite industry as a whole combined for revenues in excess of $85 billion (US). However, one of the major barriers to further access to space remains the prohibitive cost of launching payloads into orbit. In 1997 NASA released their Highly Reusable Space Transportation Study which stated that they would like to see the cost of launching 9,000 – 18,000 kg of payload into Low Earth Orbit (≈270 km) be reduced from the then price of approximately $22,000/kg (≈$10,000/lb) to near $220/kg - $440/kg ($100/lb - $200/lb) by 2010 (this date has since been revised to 2025). One of the main candidates for achieving this aggressive goal was identified as air-breathing rocket technologies, collectively known under the acronym RBCC (*R*ocket *B*ased *C*ombined *C*ycle) engines.

The typical RBCC operating cycle consists of three to four distinct operating modes: (1) ejector; (2) ramjet; (3) scramjet; and (4) rocket; where depending on the overall engine design the scramjet cycle may or may not be present. Of critical importance during the low speed, low altitude phases of launch is the ejector operating mode, where the entrainment and subsequent compression of the atmospheric air is largely responsible for any increased performance over traditional rockets. This is accomplished within the ejector section of the engine (Fig. 1), where the high energy rocket exhaust transfers both its momentum and energy to the entrained air stream.

This mixing and compression process within various types of ejectors has been the subject of research dating back as early as 1949 with the work of Von Karman [1]. Thrust augmenting ejectors, even in applications where they are not part of a combined cycle engine, have been shown to have the potential to improve performance. From a theoretical viewpoint, Alperin and Wu [2] studied simplified constant area ejectors which act to entrain and mix atmospheric air with a primary jet. After expanding the flow to atmospheric pressure, they show that when compared to the thrust of the primary jet alone (expanded to the same pressure) one can achieve appreciable

levels of increased thrust. Dutton and Carroll [3] also consider a similar ejector configuration but with emphasis on optimizing not the overall thrust augmentation, but rather on optimizing some of the more common ejector operating parameters within a combined cycle engine. These include maximizing the ratio of entrained air to primary jet mass flows (α), minimizing the ratio of primary jet to entrained air total pressures (ξ), or maximizing the ratio of exit to entrained air total pressures (π_e).

The incorporation of the ejector within the larger class of RBCC engine technologies has been examined by numerous other researchers over recent years (e.g., Daines and Segal [4], Billig [5], Fink [6], Ramette et al. [7], Han et al. [8]). However, during the 1960's while under contract to NASA the companies of Marquardt, Rocketdyne, and Lockheed combined to produce a nine volume report detailing numerous combined cycle propulsion systems as possible alternatives to the then under consideration Space Shuttle. Much of the current RBCC research can be shown to have roots in this report and the subsequent dissemination of its contents. For example, the concentric annular rocket configuration studied by Daines and Merkel [9] is a simplification of the dual concentric annular rocket configuration used in the Super-charged Ejector Ramjet described by Escher [10], while the Strutjet design of Bulman and Siebenhaar at Aerojet [11,12] is similar to the layout chosen for what Escher refers to as the ScramLACE (*SCRAM*jet *L*iquid *A*ir *C*ycle *E*ngine) Synerjet design (both engine concepts being those identified in the report as being most worthy of further investigation and development).

Although almost all research in the area of RBCC design acknowledges that the rocket configuration within the ejector duct can have a significant impact on overall performance, there is little in the way of quantitative evidence testifying to this effect. At the Pennsylvania State University, Cramer et al. [13] compared the effect of using twin thrusters to a single thruster within a rectangular ejector geometry. Although this study found that the twin thruster configuration could entrain more air, mix in a shorter distance, and produce higher compression ratios than the single thruster, only a single twin thruster configuration was examined.

Daines and Merkle [9] use a pressure based, finite difference algorithm solving the Favre averaged Navier-Stokes equations closed by the kε turbulence model of Chen and Kim to examine an axisymmetric configuration in which both a single rocket along the duct centreline and an annular rocket placed so as to evenly divide the air flow are compared. Here again, although results show a significant increase in the mixing rate using the annular rocket configuration, only a single annular configuration is examined while parameters such as downstream fuel injection and flight Mach number are varied to test their effects on the single central rocket configuration.

Rocket configuration was also identified as a means of improving ejector performance by Makaron and Fedyayev [14], where not only the placement of the nozzles, but the angle of their exhaust relative to the entrained air was examined. This idea is similar to that used at the Brigham Young University by Daines [15] and Daines and Bulman [16], where a straight, rectangular ejector was examined. However, as opposed to simply fixing the rocket exhaust angle for a given configuration, a Crank-Nicholson scheme was used to obtain time accurate solutions involving the dynamic switching of the rocket exhaust angle. In addition to increases of up to 52% in the level of thrust, it was also reported that the dynamic operation of the ejector increased the entrained air mass flow rate by nearly 75% compared to a steady flow ejector.

Various other numerical simulations of ejectors and/or ducted rockets have been performed (Matesanz and Velazquez [17], Ristori and Dufour [18], Steffen et al. [19], Stowe et al. [20], and Vanka et al. [21]), all of which share two common properties with most of the studies mentioned thus far. In each case, only a single rocket exhaust configuration is examined within a constant area ejector. It is the objective of this paper to consider an

axisymmetric ejector and vary the rocket exhaust configuration to quantify the effect this has on two key ejector performance criteria: (a) the overall mixing of the rocket and air streams and (b) the overall compression ratio of the ejector (π_e).

In furtherance of the second criteria, it is noted that most of the research aimed at improving ejector performance has dealt with constant area ejectors. However, some researchers (Makaron and Fedyayev [14], Escher [10]) have noted that the ejector duct itself can be modified to potentially improve performance. Therefore, it is also the objective of this paper to show that exit area constriction can be used to effectively increase the compression ratio of a constant length axisymmetric ejector. Both the degree to which the area is constricted and the manner in which this constriction is performed are shown to have a significant positive impact on the overall compression ratio.

2 Numerical Solution

The axisymmetric, multi-species, *F*avre *A*veraged *N*avier-*S*tokes (FANS) equations combined with the Wilcox kω turbulence model (including the Wilcox dilatational dissipation correction) are solved in generalized curvilinear form using WARP (*W*indow *A*locatable *R*esolver for Propulsion). This code uses an implicit Euler time marching scheme incorporating block implicit factorization to iterate towards a steady state solution using a pseudo-time step determined from a combination of both the minimum and maximum CFL based local time step conditions. The convective terms are treated using the Roe scheme in conjunction with Yee flux limiters while the diffusive terms are treated with a second order accurate, centered, finite difference stencil. Convergence is evaluated using the magnitude of both the continuity and energy residuals, where a solution is judged converged when the residual has been reduced by approximately eight orders of magnitude. Details of the code and its validation on both axisymmetric and non-axisymmetric high speed flows can be found in Refs. [22,23,24]

For all the configurations presented, the results are obtained on a two dimensional grid approximately 600 x 150, with clustering around the rocket walls protruding into the ejector section. For the conical/cylindrical configurations, clustering at the location where the configuration changes from conical to cylindrical is added such that a streamwise grid spacing of approximately 1 mm is obtained. A grid convergence study was done for the constant area central/annular ejector configuration in this paper (see Ref. [24]) where it was found that although differences of approximately 10% were seen between the mass flow averaged compression ratios in going from a grid of dimensions 517 x 150 to 2000 x 450 (an eleven fold increase in grid density), this error was on the conservative side in that the smaller grid under predicted π_e.

The total length of all the ejectors considered is 1.0 m while the outer diameter at the ejector inflow plane is 0.2 m. Both the total pressure and total temperature are held constant at the air inflow boundary thus allowing the inflow Mach number to change, which in turn leaves the air mass flow rate free to adjust to the ejector flow field. The rocket exhaust inflow boundary is supersonic with the Mach number, static pressure, and static temperature specified. The outer wall of the ejector, as well as the 10 mm sections of rocket wall protruding into the ejector section, are specified as no-slip, adiabatic walls while the central axis boundary is symmetric. To avoid dividing by zero near the axisymmetric axis, an offset of 0.01 micrometers is applied along the length of the ejector. In cases where the overall ratio of air to rocket exhaust mass flows is kept constant, the static pressure is specified along the entire height of the ejector outflow plane so as to produce a value for α as close as possible to 0.75 (for all other cases no conditions are specified at the outflow). On a massfraction basis the air is modeled as 77% N_2, 23% O_2 while the rocket exhaust is composed of 76% O_2, 17% CO_2, and 7% H_2O. This corresponds

to an equilibrium post combustion mixture for kerosene and oxygen at an equivalence ratio of 0.2 based on the reaction,

$$\phi C_{12}H_{24} + 18O_2 \rightarrow 12H_2O + 12CO_2 \quad (1)$$

The equivalence ratio is chosen such that no combustible species enter the ejector thereby eliminating the possibility of simultaneous mixing and combustion. The turbulent Schmidt and Prandtl numbers are set to 1.0 and 0.5 respectively, while the freestream value of ω is set to ten times the flow speed (both Pr_T and Sc_T along with the wall value of ω are set to the values recommended by Wilcox [25]).

3 Rocket Exhaust Configuration

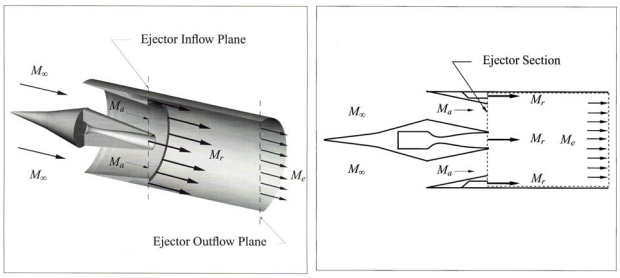

Fig. 1 Central/Annular Configuration

For the ejector section of an RBCC engine to be effective, it must obtain two key objectives. The first, and most fundamental objective, is that the flow at the exit plane be as close to fully mixed as possible. Since the majority of the energy input into the ejector is initially contained within the rocket stream alone, efficient mixing is required to transfer this energy to the entrained airstream (additionally, for cases in which both mixing and combustion are occurring within the ejector section, a greater degree of mixing promotes a more uniform fuel/air ratio over a larger region). The second fundamental objective, that which provides the major measure of performance, is that the total pressure of the mixed flow at the exit plane be increased from that of the entrained air. An effective ejector section will achieve both of these goals, since both a fully mixed exit flow at a low total pressure or an exit flow with a limited high total pressure region will not result in acceptable levels of overall engine performance.

In order to evaluate the effect of rocket placement on these objectives, two simple configurations are examined. The first uses a single rocket placed along the axisymmetric axis of a constant area ejector while the second, shown in Fig. 1, adds an annular rocket along the outer wall of the ejector section. Two central/annular configurations are compared to the single central rocket case, one in which the rocket exhaust entering the ejector is split evenly between the two rocket streams, the other with the annular rocket containing 75% of the total rocket exhaust entering the ejector.

The flight conditions are constant for all the cases considered in this paper, with the ejector operating at an altitude of 6.3 km and a flight Mach number of 0.8. Both the air and rocket conditions at the ejector inflow plane are listed in Table 1.

The case of the single central rocket configuration is shown in Fig. 2(a), where the nitrogen massfraction contours (with Mach numbers overlaid) are shown above Mach number profiles taken across the upper portion of the axisymmetric ejector at various downstream locations within the constant area duct. As can be seen, there is very little penetration of the rocket exhaust into the airstream (or vice versa), where even at the 100 cm location the Mach number profile shows a very distinct high Mach region below a radius of approximately 5 cm, indicative of a purely rocket exhaust flow. The only real mixing occurs within the shear layer, which as shown by the nitrogen contours, has only limited success in mixing the two streams.

Table 1 Ejector Inflow Conditions

p_a^o	58.7 kPa
T_a^o	267 K
p_a^o / p_∞^o	0.85
p_r^o	5870 kPa
T_r^o	2316 K

The same results for the two central/annular configurations examined are shown in Fig. 3(b) and 3(c). In these cases there is a clear improvement in the manner in which the air and rocket exhaust mix, where although there is still a discernable pure rocket core along the central axis, the contours in the outer regions show the presence of nitrogen at the ejector wall indicating the absence of a pure rocket stream anywhere but within the narrow region near the axis. This is confirmed by the Mach number profiles, where the high Mach number rocket exhaust visible at the outer wall of the ejector entrance is absent at the 100 cm location in both annular rocket configurations.

Also interesting to note is the location at which the entrained air reaches sonic velocity. Where the air flow in the single central rocket configuration reaches M=1 within approximately 25 cm, the presence of an annular rocket stream more than doubles this distance. Comparing Figs. 3(a) and 3(c) one can see that when present, the annular rocket stream undergoes several expansion/ compression cycles during the same distance the central stream undergoes a single cycle. This increases the degree to which the annular rocket exhaust and air streams mix, to the point that by the time the entrained air reaches sonic velocity one can no longer reasonably assume a zero thickness shear layer between the two streams (as there is no longer a distinct annular rocket stream). This gives rise to the slight differences in α shown in Table 2, where both the area of the entrained air streamtube and the degree of mixing experienced up to the choke point, determine the mass flow of air capable of being passed through the ejector section (recalling that the rocket exhaust mass flow is fixed).

In terms of achieving the first fundamental objective of an efficient ejector, that of effectively mixing the rocket and air streams, it is clear that the central/annular configurations result in the best levels of mixing. However, as seen in Fig. 3(c), the $75_a/25_c$ configuration has the most uniform Mach number profile over the largest area, with a greater quantity of the exit flow at the mixed flow Mach number.

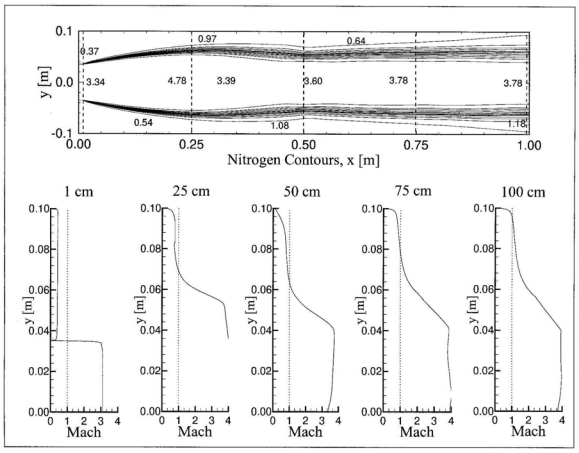

(a) $0_a/100_c$

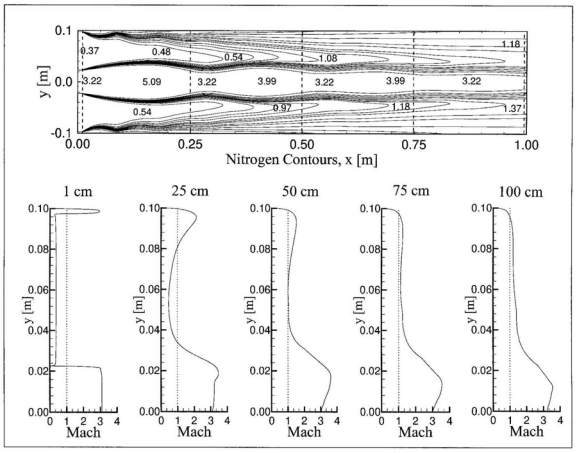

(b) $50_a/50_c$

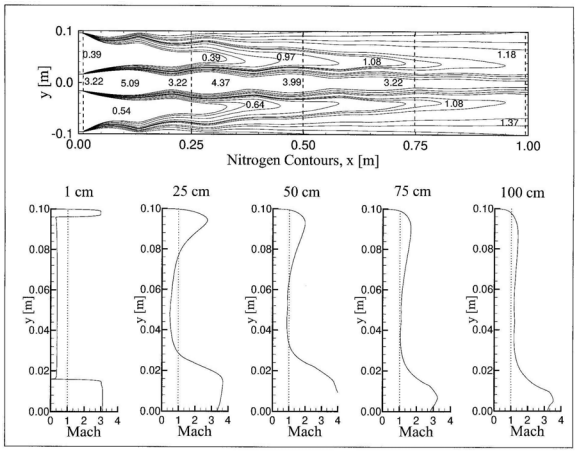

(c) $75_a/25_c$

Fig. 3 Central/Annular Ejector Flow Fields

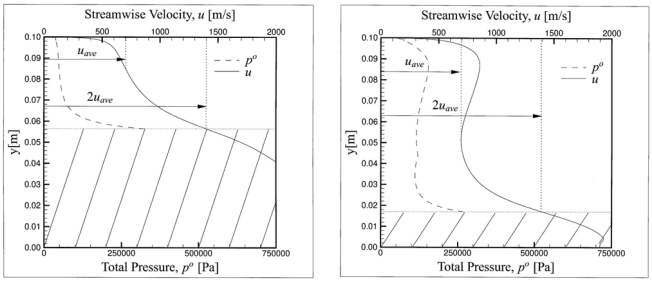

(a) $0_a/100_c$ **(b) $75_a/25_c$**

Fig. 3 Determination of Mixed Flow Regions

In terms of evaluating the compression ratio, the presence of a pure rocket core along the axisymmetric axis can bias the results towards configurations with larger cores, as the exhaust total pressure is initially 100 times that of the incoming air. Therefore, after determining the mixed flow velocity the radius at which this speed is double is determined. Given that the highest streamwise velocities occur along the axis at the centre of the rocket core, as the radial distance increases, the streamwise velocity decreases until it reaches double the mixed flow velocity. The total pressure is then calculated on a mass flow averaged basis from this radial position outwards, thereby avoiding any artificial inflation of the compression ratio. As a consequence, for ejector configurations where the mixing is poor, a greater portion of the exit area is neglected as shown by the hatched regions in Fig. 3.

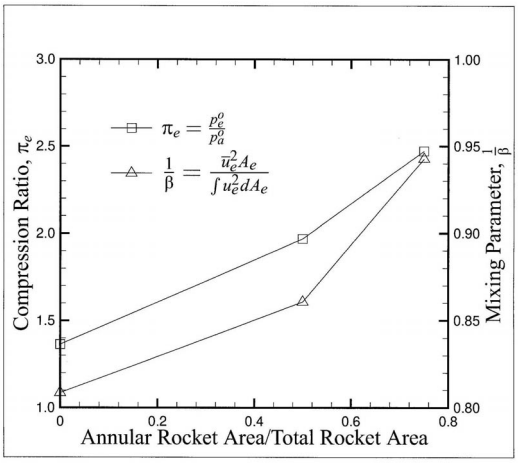

Fig. 4 Ejector Performance for Various Annular Rocket Sizes

Having defined the mixed flow regions one can calculate the compression ratios shown in Fig. 4. As can be seen, not only does the $75_a/25_c$ configuration produce the compression ratio highest in absolute magnitude (≈2.5), it also produces the most uniform profile at the 1.0 m location. This uniformity is quantified by the parameter β, where the inverse of this quantity reaches unity for a perfectly flat velocity profile. As shown, as the annular rocket area is increased, 1/β increases reflecting the diminishing size of the rocket core along the axis.

Indicative of the effectiveness of the annular rocket to impart its energy to the entrained air stream, the $75_a/25_c$ results not only show the largest compression ratio, but a value of 2.47 is only 14% below the theoretical compression ratio assuming complete mixing and no losses. As the annular rocket area decreases so does the resulting compression ratio, with the single central rocket configuration showing the worst compression at the exit plane. It should also be noted that the compression ratio of the $75_a/25_c$ configuration is based on the largest percentage of the exit area at 95%, compared to 91% and 70% for the $50_a/50_c$ and $0_a/100_c$ cases respectively.

Table 2 Ejector Exit Properties for Various Annular Rocket Sizes

Variable	$75_a/25_c$	$50_a/50_c$	$0_a/100_c$
α	1.00	0.98	1.09
M_e	1.30	1.36	1.99
π_e^*	2.47	1.97	1.36

* Mass flow averaged over mixed exit flow only, Fig. 4

4 Conical Ejector Configuration

In order to properly assess the effects of any area decrease on ejector performance, careful attention must be paid to ensuring uniformity of operating parameters between any cases being compared. Although for all of the constricted cases considered in this paper both the air and rocket conditions are held constant at the values in Table 1, this does not ensure constant ejector variables when changing the exit area. Since a decrease in exit area will

decrease the allowable mass flow passing through the ejector, with a fixed mass flow of rocket exhaust entering the ejector the entrained airflow must decrease to satisfy conservation of mass. A decrease in entrained airflow decreases α (where the lower this value the closer the combined cycle engine resembles a pure rocket, α=0) which has a significant impact on the compression ratio of the ejector. Independent of any effects due to area constriction, simply decreasing α (i.e., by decreasing the mass flow of rocket exhaust entering the ejector) can cause an increase in π_e. Thus if α is not kept constant between cases being compared, any increases observed in π_e could not be positively attributed to the effects of exit area constriction.

Therefore, since the maximum total mass flow through the ejector occurs when the mixed flow at the exit reaches sonic velocity, the maximum constriction ratio is chosen such that when operating at this critical condition α=0.75. For all lesser degrees of constriction, the exit pressure is set to a value which produces the same value for α as the maximum constriction case but which is generally above that required to choke the flow at the exit.

Figure 5(a) shows the first constriction strategy considered, a conically constricting duct where the outer wall angle is set so that the desired area is obtained at the exit plane of a 1.0 m ejector. For the three constriction ratios considered (12%, 21%, and 25%), Fig. 5(b) shows the increase in the mixed flow Mach number required to maintain α=0.75 as the exit area is decreased.

As shown, the mixed flow Mach number for the case with the highest degree of constriction is approximately constant at a value of unity, which indicates that this configuration is operating under maximum mass flow conditions. Thus cases in which the exit area is constricted by more than 25% are not considered as it is impossible to set the ratio of air to rocket exhaust mass flows at 3:4 for the operating conditions listed in Table 1. Also shown in Fig. 5(b) is the Mach number profile of the constant area configuration operating at α=0.75, where on a mass flow averaged basis the Mach number is now 0.53 as compared to the value shown in Table 2 of 1.30 (where no exit plane conditions are specified).

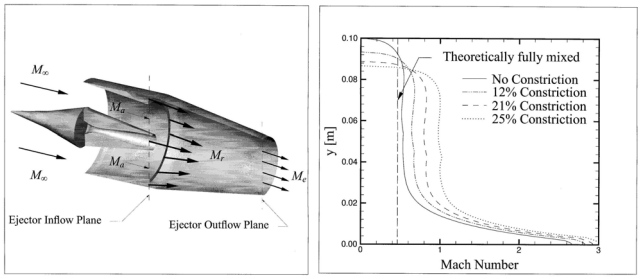

(a) **(b)**

Fig. 5 Conically Constricting Ejector

Calculating the mixed flow regions as done previously results in the augmentation of the ejector compression ratios shown in Fig. 6(a). As can be seen, increasing the degree of constriction increases the compression ratio exponentially, where despite smaller incremental decreases in exit area the compression augmentation more than doubles between consecutive cases considered (the compression augmentation, Π_e, is simply the compression ratio of the constricted configuration divided by that of the constant area configuration). Although the effect of the exit area decrease on Π_e is minimal for a 12% constriction (approximately 4%), for the case in which the exit flow reaches sonic velocity the compression ratio increases by approximately 23%.

Figure 6(b) compares the resulting compression ratio profiles at the ejector exit plane for all the degrees of constriction considered (from which the results in Fig. 6(a) are determined). As shown, the size of the central rocket exhaust stream at the exit plane is approximately independent of the degree to which the exit area is decreased. This indicates that the central rocket core contains nearly the same quantity of energy in each case and that the observed increases in the compression ratio are thus not due to a more efficient transfer of energy to the mixed flow. However, examining the relationship between the boundary layer

height (δ) and the decrease in exit area in Fig. 6(a), it is observed that the greater the degree of area constriction, the smaller the resulting boundary layer at the exit plane. Therefore, for cases where the angle of the outer wall promotes the annular rocket stream's penetration into the entrained air stream, more of its energy is observed to be transferred to the mixed flow region as opposed to being consumed by viscous losses near the wall. Thus although the outer wall angle has little effect on the central rocket core, its effect on the annular rocket stream is more pronounced. It should also be noted that the decrease in boundary layer height is not an effect of decreasing the length of the surface along which the boundary layer develops, as for each degree of constriction the outer wall angle is varied (from 0.70° for a 12% constriction to 0.85° for a 25% constriction) to achieve the desired exit area over a constant length of one meter.

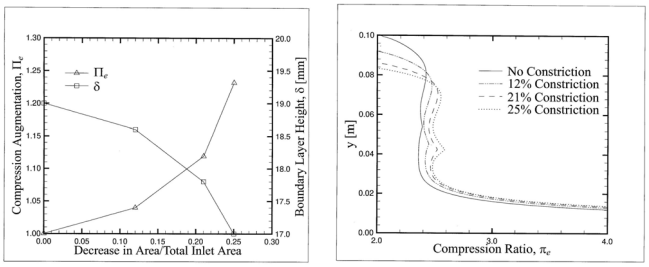

(a) **(b)**

Fig. 6 Conical Constriction Results

5 Conical/Cylindrical Configuration

For all the variable area configurations considered thus far, constriction has occurred over the length of the entire ejector as shown in Fig. 5(a). However, for a given constriction ratio the outer walls can be more severely angled to yield the required area over a length significantly shorter than the total ejector length itself. For a constant length ejector this yields the conical/cylindrical, or funnel, configuration shown in Fig. 7.

In order to evaluate the effects of using a constant area cylindrical section in combination with a conically converging length, the $75_a/25_c$ configuration with a 25% area constriction is used. Cylindrical lengths of 13 cm, 18 cm, and 25 cm are placed downstream of the conical section thereby creating ejectors which constrict over 87%, 82%, and 75% of their lengths respectively.

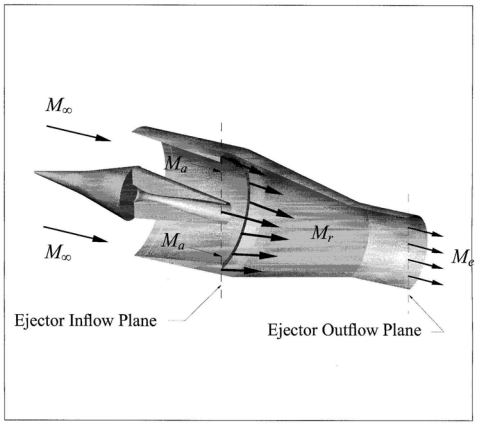

Fig. 7 Conical/Cylindrical Configuration

The Mach number contours for both the shortest and longest cylindrical sections are shown in Fig. 8. It should be noted that the third and fourth profiles are at different locations between Figs. 8(a) and 8(b), where in each case the profile is located at the beginning and midpoint of the cylindrical section (which occurs at different streamwise distances depending on the length of the conical section). Examining the profiles at both the 87 cm and 75 cm locations in Figs. 8(a) and 8(b) respectively, it is observed that the mixed flow makes the transition to completely sonic velocity at the beginning of the cylindrical section in each case independent of the streamwise location. As shown, the flow is approximately choked across the entire height, with only a small region of high subsonic flow existing between radii of approximately 3 cm and 6 cm. Also interesting to note, the profiles at these locations appear independent of the length of the cylindrical section considered, despite the fact that the entrance to the longest section is located twice the distance from the ejector exit plane as compared to the entrance of the shortest section.

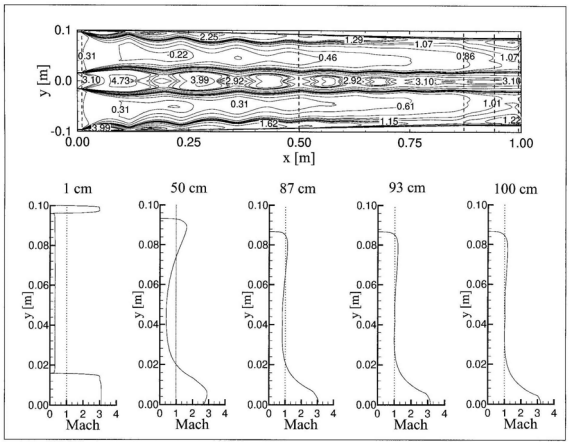

(a) 13 cm

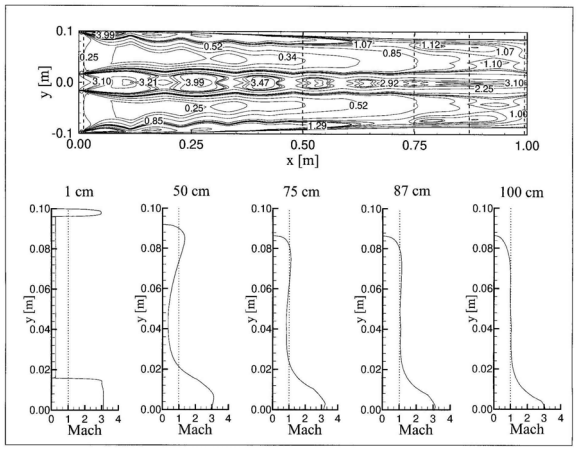

(b) 25 cm

Fig. 8 Conical/Cylindrical Ejector Flow Fields

The most significant impact of this result is shown in the Mach number contours at the ejector entrance, where at the 1 cm location the 13 cm configuration produces an air inflow Mach number of 0.31, approximately 24% higher than the value of 0.25 shown for the 25 cm configuration.

As shown in Table 3, this results in a variation of α by as much as 15% from the case where the constriction takes place over the entire length of the ejector. This is a direct result of the exit plane being isolated from the upstream portions of the flow by the critical condition at the entrance to the cylindrical section. Since the flow at this point has already reached sonic velocity, any downstream boundary conditions imposed at the exit serve only to alter the flow within the cylindrical, or isolator, section itself. Therefore, the conditions at the air inflow plane are determined by the throat location as seen by the subsonic flow, which for all isolator lengths occurs at the end of the conical section.

Since the degree to which the two streams have mixed before reaching the critical location depends on the length of the conical section, each isolator length produces a different value of α. However, since an increase in the air/rocket mass flow ratio tends to decrease the compression ratio, the variations observed for both the 13 cm and 18 cm isolators add a conservative effect when evaluating the compression ratio of these configurations (while the 25 cm isolator configuration produces a value less than 3% below that observed for the purely conical ejector).

Table 3 Ejector Exit Properties for Conical/Cylindrical Configurations

	0 cm	13 cm	18 cm	25 cm
α	0.75	0.86	0.82	0.72
M_e	0.96	1.14	1.13	0.96
π_e	2.47	2.92	2.90	2.85

Figure 9 shows the compression augmentation results for both the conical and conical/cylindrical ejector configurations. One of the most interesting results is that it is the shortest isolator length which produces the highest compression augmentation, 30% higher than a similar ejector without any area constriction and still 7% higher than a conical configuration with the same degree of constriction. This is despite the fact that the air/rocket mass flow ratio is nearly 15% higher when using the 13 cm isolator as compared to the conical configuration, a factor which acts to decrease the resulting compression ratio. The augmentation values for the 18 cm and 25 cm isolators are also nearly 30% (29% and 27% respectively), indicating that although the longer cylindrical lengths produce a larger boundary layer which tends to decrease π_e, this effect is approximately offset by the increase in π_e due to the decrease in α. Therefore, for the isolator

length at which the air/rocket mass flow ratio more closely matches the value obtained using a purely conical configuration, one can expect an additional 5%-7% increase in the compression ratio.

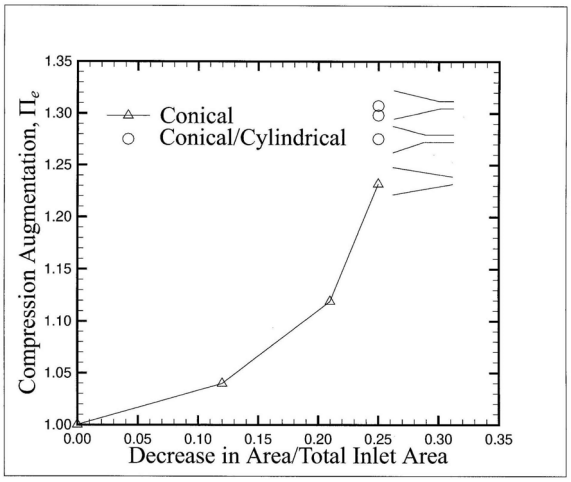

Fig. 9 Constricted Ejector Performance

6 Conclusions

The use of an ejector configuration which has 75% of the rocket exhaust enter the ejector through an annular stream along the outer wall dramatically increases both the rapidity of the mixing process within the ejector and the degree of mixing obtained at the exit. For the given flight and rocket conditions, this translates into a mixed flow extending across 95% of the total exit area with a total pressure nearly two and a half times that of the entrained air when both the air and rocket exhaust mass flows are equal. These results also indicate that it is the annular rocket stream which mixes best with the entrained air, where only the central rocket stream is still identifiable at the ejector exit.

It is further shown that exit area constriction can be used to increase the resulting compression ratio. An area decrease of 25% the inlet area over the entire length of a 1.0 m ejector is shown to produce a 23% increase in the compression ratio (over that obtained using an unconstricted configuration under the same operating conditions). However, it should be noted that the degree of constriction is limited by the associated decrease in the entrained air mass flow rate and the minimum required α.

The manner in which the area is decreased is also shown to have an impact on the compression ratio. Results indicate that there exists an optimum length somewhere between 75% and 82% of the total ejector length over which the area should be decreased. Using a cylindrical section over the remaining length can yield an additional 5%-7% increase in the compression ratio over a purely conical ejector of equal length and decrease in area. Also, the cylindrical section is found to act as an isolator between the outflow and inflow boundaries, where it is found that the mixed flow chokes at the end of the conically constricting area independent of the length of the cylindrical section, where conditions at this location control the overall air/rocket mass flow ratio.

Acknowledgements

This work was sponsored by the Natural Science and Engineering Research Council of Canada. Thanks must also be extended to B. Parent at Seoul National University for the extensive use of the WARP code.

References

[1] von Karman, Theodore. Theoretical remarks on thrust augmentation, *Reissner Anniversary Volume: Contributions to Applied Mechanics*, edited by P.I. of Brooklyn, J.W. Edwards, Ann Arbor, Michigan, 1949. pp. 461-468.

[2] Alperin, M and Wu, J. Thrust augmenting ejectors, part I, *AIAA Journal*, Vol. 21, No. 10, 1983, pp. 1428-1436.

[3] Dutton, J and Carroll, B. Optimal supersonic ejector designs, *Journal of Fluids Engineering*, Vol. 110, December 1986, pp. 414-420.

[4] Daines, R and Segal, C. Combined rocket and airbreathing propulsion systems for space launch applications. *AIAA Journal of Propulsion and Power*, Vol. 14, No. 5, 1998, pp. 605-612.

[5] Billig, F S. Developments in high-speed-vehicle propulsion systems, Vol. 165 of *Progress in Astronautics and Aeronautics (Chapter: Low speed operation of an integrated rocket-ram-scramjet for a*

transatmospheric accelerator), AIAA, 1996, pp. 51-103.

[6] Fink, L E. Tactical missile propulsion, Vol. 170 of *Progress in Astronautics and Aeronautics, (Chapter: High Mach Number Applications: Combined Cycles)*, AIAA, 1994, pp. 497-515.

[7] Ramette, P, Scherrer, D, and Doublier, M. Etude comparative de differents systemes de propulsion combinee, *AGARD Conference Proceeding 479*, 1990.

[8] Han, S, Peddieson, J, and Gregory, D. Ejector primary flow molecular weight effects in an ejector-ram rocket engine, *AIAA Journal of Propulsion and Power*, Vol. 18, No. 3, 2002, pp. 592-599.

[9] Daines, R L and Merkle C L. Computational analysis of mixing and jet pumping in rocket ejector engines, AIAA Paper 95-2477, 1995.

[10] Escher, W J. Synerjet for earth/orbit propulsion: revisiting the 1966 NASA Marquardt composite (airbreathing/rocket) propulsion system study, SAE Paper 851163, May 1985.

[11] Siebenhaar, A and Bulman, M. Application and testing of rocket based combined cycle engines for missile propulsion, *32nd JANNAF Combustion Subcommittee Meeting and Propulsion Engineering Research Center 7th Annual Symposium*, JANAAF, 1996, pp. 271-284, N1996-27892.

[12] Siebenhaar, A and Bulman M. Strutjet matures to support propulsion need in the 2000+ world, ISABE Paper 99-7217.

[13] Cramer, J M, Greene, M, Pal, S, and Santoro, R J. RBCC ejector mode operating characteristics for single and twin thruster configurations, AIAA Paper 2001-3464, 2001.

[14] Makaron, V and Fedyayev, Y G. Organization of working process in liquefied air cycle rocket-ramjet engine, AIAA Paper 96-4522.

[15] Daines R L. Numerical analysis of high-frequency jet-switching on dynamic ejector flow fields, AIAA Paper 97-2757.

[16] Daines, R L and Bulman, M. Computational analyses of dynamic rocket ejector flow fields, AIAA Paper 96-2686.

[17] Matesanz, A, Velazquez, A, Tizon, J, and Montanes, J. Numerical reconstruction of ejector rocket experimental tests, *AIAA Journal of Propulsion and Power*, Vol. 18, No. 6, 2002, pp. 1191-1198.

[18] Ristori, A and Dufour, E. Numerical simulation of ducted rocket motor, AIAA Paper 2001-3193.

[19] Steffen Jr, C L, Smith, T, Yungster, S, and Keller, D J. Computational analysis for rocket-based combined cycle systems during rocket-only operation, *AIAA Journal of Propulsion and Power*, Vol. 16, No. 6, 2000, pp. 1030-1039.

[20] Stowe, R, Dubois, C, Harris, P, Mayer, A, Champlain, A D, and Ringuette, S. Two phase flow combustion modeling of a ducted rocket, AIAA Paper 2001-3461.

[21] Vanka, S, Craig, R, and Stull, F. Mixing, chemical reaction, and flow field development in ducted rockets, *AIAA Journal of Propulsion and Power*, Vol. 2, July 1986, pp. 331-338.

[22] Parent, B and Sislian, J P. Validation of the Wilcox kω model for flows characteristic to hypersonic airbreathing propulsion, *AIAA Journal*, Vol. 24, No. 2, 2004, pp. 261-270.

[23] Etele, J. Computational study of variable area ejector rocket flow fields, PhD. thesis, University of Toronto, Institute for Aerospace Studies, 2004.

[24] Etele, J, Sislian, J P, Parent, B. The Effect of Rocket Exhaust Configurations on the Ejector Performance of an RBCC engine. *Journal of Propulsion and Power*, (submitted May, 2004).

[25] Wilcox, D C. *Turbulence modeling for CFD*, DCW Industries, Inc., 2nd ed., 1998.